stage III in aluminum is due to the migration of single vacancies to interstitial agglomerates formed during the preceding stages of recovery. These interstitial clusters must be stable at least beyond the point where the deepest of the impurity traps release their interstitials. The impurity atoms can delay the diffusion of a vacancy migrating through the lattice by causing the defect to make more jumps, on the average, before annihilation. The presence of the impurities does not affect the activation energy for the onset of vacancy migration. Impurities can also trap the migrating vacancies and subsequently release them at a temperature well above that where the initial vacancy migration occurs. In light of the data presented in this research it is felt that the introduction of a second type of interstitial that moves in stage III is not necessary to explain the results.

## ACKNOWLEDGMENTS

The authors wish to thank Dr. C. L. Snead, Jr., for many helpful suggestions during the course of this work. One of the authors (P.B.P.) wishes to thank the Virginia Military Institute for financial support during the period of this research.

PHYSICAL REVIEW VOLUME 174, NUMBER 3 15 OCTOBER 1968

# Lattice Thermal Conductivity, Nernst-Ettinghausen Effect, and Specific Heat in Antimony at Low Temperature*

R. S. BLEWER,† N. H. ZEBOUNI, AND C. G. GRENIER
*Louisiana State University, Baton Rouge, Louisiana 70803*
(Received 5 July 1967; revised manuscript received 3 May 1968)

The lattice thermal conductivity, the high-field Nernst-Ettinghausen thermoelectric coefficient, and the specific heat of antimony have been determined in the temperature range 0.4–2.4°K. Thermal-conductivity results confirm the predominance of phonon-electron normal scattering in the lowest range of temperatures with the expected $T^2$ law. The dramatic increase in the lattice thermal conductivity above 1.5°K is thought to be due to the inability of the electrons to scatter phonons with wave numbers $q>2k_F$, where $2k_F$ is the diameter of a charge carrier's Fermi pocket. An effective scattering Debye temperature of $\Theta^*=(2k_F/q_D)\Theta \approx 25$°K is in good agreement with experimental results. Nernst-Ettinghausen results give the total electronic density of states $Z=(1.10\pm0.07)\times10^{33}$ erg$^{-1}$ cm$^{-3}$; the presence of a phonon-drag contribution is confirmed and discussed. The specific-heat results, $C=(116.5\pm6.4)T+(211.0\pm5.3)T^3+1.97\pm0.23)T^{-2}$ in $\mu$J (mole °K)$^{-1}$, are compared with the results of transport measurements and with recent specific-heat determinations.

## I. INTRODUCTION

PART of this work is an extension to lower temperatures of Long, Grenier, and Reynolds's[1] study of the transport properties of antimony with the purpose of clarifying the nature of the scattering mechanisms.

A case in point relates to the Nernst-Ettinghausen (NE) effect and how precise a determination of the electronic density of states, $Z$, can be achieved from it. Their results indicated the existence of a strong superimposed phonon drag which prevented the electronic term from being determined with sufficient accuracy. To improve on this point, measurements of the transport effects were extended down to 0.4°K. Also, an independent determination of the density of states was made through specific-heat measurements in this same range of temperature.

Another point pertained to the inability to work out a scheme which would explain most properties related to the phonon system. For example, the magnitude and temperature dependence of the lattice thermal conductivity $\lambda_g$ and the ideal electronic conductivity $\sigma_i$ were found to disagree with Makinson's[2] and with Debye, Grüneisen, and Bloch's[3] formulas for metals, but the ratio between these two quantities agreed remarkably well with Ziman's $T^7$ law,[4] strongly indicating the predominance of phonon-electron scattering. Even though this conclusion seems reasonable, the strong three-phonon normal process implied in Ziman's theory is not very likely at these low temperatures. For that reason the extension of the measurement of $\lambda_g$ down to 0.4°K was desirable in order to better understand the phonon scattering processes. A better understanding of the phonon drag also can be attained.

Section II presents briefly the pertinent details of the experimental procedure; Sec. III presents the results and discussion of the thermal-conductivity measurements, the NE effect, and the specific heat. Section IV

* Work performed under the auspices of the U. S. Atomic Energy Commission and is Report No. ORO-3087-26 under Contract No. AT-(40-1)-3087.

† Present address: Electronic Components Laboratory, U. S. Army Electronics Command, Ft. Monmouth, N. J.

[1] J. R. Long, C. G. Grenier, and J. M. Reynolds, Phys. Rev. **140**, A187 (1965); Phys. Letters **16**, 214 (1965).

[2] R. E. B. Makinson, Proc. Cambridge Phil. Soc. **34**, 474 (1938).

[3] J. M. Ziman, *Electrons and Phonons* (Oxford University Press, London, 1960), p. 364.

[4] J. M. Ziman, *Electrons and Phonons* (Oxford University Press, London, 1960), pp. 319–322.

draws the conclusion of this study. The effect of the Landau quantization on the transport effects is not included in this paper.

## II. EXPERIMENTAL DETAILS

A $He^3$ refrigerator similar to the one described by Reich and Garwin[5] was used. The lowest temperature attainable was about 0.7°K in continuous operation and 0.36°K in batch operation. Regulation of the $He^3$ bath temperature could be maintained in the continuous mode of operation by adjusting the opening of a bypass valve between intake and output of the $He^3$ forepump. In batch operation, an electric heater feedback system similar to the one described by Forstat and Novak[6] was used to control the temperature in the region below 0.7°K. This method could achieve a stability of 1 mdeg over a 30-min period. Very pure $He^3$ gas was used (vapor pressure standard) and the secondary thermometers (Allen-Bradley 10-Ω, $\frac{1}{10}$-W resistors) were calibrated directly against the vapor pressure of the $He^3$ bath. The best conditions for calibration were obtained by pumping the system to the lowest temperature attainable, then shutting off the $He^3$ system completely from the outside; the system then warmed up slowly over a period of 2–3 h, during which the calibration of the thermometers versus the slowly rising vapor pressure was carried out. The over-all extraneous heat leak to the sample, sample holder, and $He^3$ cryostat was estimated to be about 50 $\mu$W. The instrument used to measure the vapor pressure of the $He^3$ was a quartz Bourdon tube manufactured by Texas Instruments Incorporated. The tube range was 0–200-mm Hg, and its sensitivity was about 1% in the 100-$\mu$ region and 0.1 % in the 1-mm region. At the lowest temperatures a correction to the pressure readings was made[7] to take into account the thermomolecular effect. The whole calibration procedure was found to be very reproducible. It was found that the use of epoxy resin seals in contact with the $He^3$ evaporator was to be avoided because their high heat capacity and extremely low thermal conductivity make their cooling down to an equilibrium temperature extremely slow and can disrupt the secondary thermometer calibration.

The transport measurements and the crystal used have been fully described by Long *et al.*[1] The magnetic field was applied along the trigonal [111] (or $z$) direction and the transport effects were measured in the (111) (or $x$-$y$) plane. The single crystal has a resistivity ratio $\rho_{300}/\rho_{1.2}\simeq 9000$ with a residual resistivity $\rho_0 \simeq 5\times 10^{-9}$ Ω cm. For the measurement of the isothermal electrical magnetoresistivity $\rho_{11}$, a current of 1.2 mA was used. $\rho_{11}$ was found to be nearly independent of $T$ below 2°K.

For the temperature measurement in the low range of temperatures investigated it was found that 10-Ω, $\frac{1}{10}$-W Allen Bradley resistors had the proper sensitivity. At temperatures below 0.9°K it was found necessary to limit the thermometer current to 0.2 $\mu$A if self-heating effects were to be avoided. Under these conditions, the thermometers were found to obey very accurately a relation between their resistance $R$ and the vapor pressure $P$ of the $He^3$ liquid given by[8] $\log R = a + \sum_n b_n \times (\log P)^n$. Heat currents for the thermomagnetic phenomena ranged from 0.5 $\mu$W at 0.44°K to 150 $\mu$W at 2.3°K; care was taken to keep the temperature gradient sufficiently small (<0.1°K/cm) to allow the use of linear approximations in the computations.

A different sample and sample holder were used for the specific-heat measurements. The sample was a 142.429-g bar of antimony cut from the same parent bar from which the crystal was obtained for the transport measurements. The sample was soldered to the base of a platform suspended from the evaporator of the $He^3$ refrigerator by three 3-mm-diam graphite rods[9] 5 cm long; the rods served as heat shunts during precooling, circumventing the need for helium exchange gas. A 0.001-in.-diam 99.995% pure lead wire drawn by the Wollaston process was used in conjunction with the magnetic field as a superconducting heat switch. Measurements were made by thermally isolating the sample when it had been cooled to a temperature of ~0.37°K and then supplying well-determined amounts of heat for accurately known periods of time, taking care not to change the temperature of the sample by more than 7% with each heat pulse.[10] The electronic timer used could be read accurately to microseconds and was arranged in the heater circuit so as to be automatically activated when the heater was started. The temperature of the sample was recorded as a function of time on a Brown strip-chart recorder. The technique of accounting for the heat capacity of the sample's addenda was as follows: A separate run was made in which most of the sample had been cut off with a spark cutter, and only that portion which was wetted with solder was left as part of the addenda. The measurement of heat capacity in this run was subtracted from that taken with the entire bar attached, and this difference taken as the heat capacity due to the amount (126.354 g) of pure antimony removed. The heat pulses applied ranged in power from 0.5 $\mu$W at the lowest temperatures to 6 $\mu$W near 1°K. Heating periods ranged from 2 to 6 sec depending on the criterion of less than 7% temperature rise per heat pulse stated above. The heat leak from extraneous sources to the sample was determined to be about 20 erg/min.

[5] H. A. Reich and R. L. Garwin, Rev. Sci. Instr. **30**, 7 (1959).
[6] H. Forstat and J. Novak, Rev. Sci. Instr. **29**, 733 (1958).
[7] S. G. Sydoriak and R. H. Sherman, J. Res. Natl. Bur. Std. (U. S.) **A68**, 547 (1964); T. R. Roberts and S. G. Sydoriak, Phys. Rev. **102**, 304 (1956).
[8] S. Cunsolo, M. Santini, and M. Vicentini-Missoni, Cryogenics **5**, 168 (1965); P. P. Craig, *ibid.* **6**, 112 (1966).
[9] F. J. Shore, V. L. Sailor, H. Marshak, and C. A. Reynolds, Rev. Sci. Instr. **31**, 970 (1960).
[10] N. E. Phillips, Phys. Rev. **114**, 676 (1959).

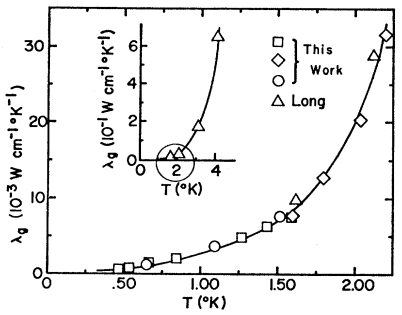


FIG. 1. Lattice thermal conductivity of Sb in the temperature range 0.4–2.4°K. The insert shows the points previously determined by Long *et al.*; circled are two points plotted with our results.

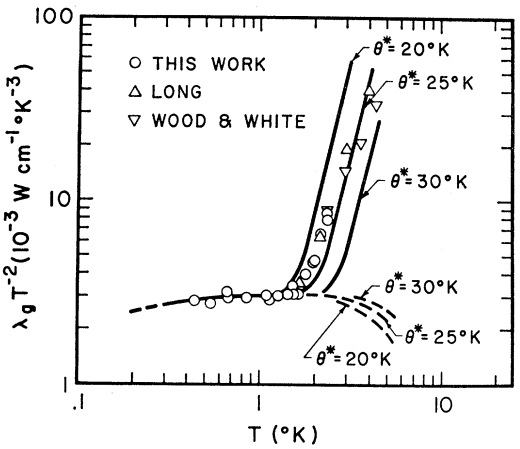


FIG. 2. The lattice thermal conductivity $\lambda_g$ of antimony, multiplied by $T^{-2}$ versus $T$ in a log-log plot. The $T^2$ dependence of $\lambda_g$ displayed below 1.4°K is due to scattering of phonons by electrons. The increase of $\lambda_g$, above 1.4°K, is due to the predominant contribution of "peripheral" phonons ($q>2k_F$). The solid curves correspond to Eq. (9) for different $\Theta^*$. The dashed curves show the contribution of phonons with $q\leq 2k_F$, Eq. (18).

## III. RESULTS AND DISCUSSION

### A. Lattice Thermal Conductivity and Phonon-Electron Normal Scattering

The thermal conductivity of antimony exhibits several interesting features at very low temperatures. In particular, the thermal magnetoresistivity $\gamma_{11}$ saturates to a constant value in presence of moderate magnetic field strengths.[1,11,12] This reflects the near-complete quenching of electronic conductivity and allows the study of the lattice conductivity and its temperature dependence. This dependence has been a matter of conjecture since the measurements of Rosenberg,[11] White and Woods,[12] and Long *et al.*[1] It was well recognized by these authors that the phonon conductivity $\lambda_g$ was mostly limited by scattering from the electrons, but the temperature dependence determined experimentally was highly anomalous: White and Woods found $\lambda_g \propto T^{3.6}$, and Long *et al.* found $\lambda_g \propto T^{4.8}$ in the temperature range $1.6\leq T\leq 4.2$°K, while a $T^2$ dependence was expected. The present work extends the thermal-conductivity measurements on the monocrystal used by Long *et al.* down to $T=0.4$°K.

Figure 1 shows the results of the lattice thermal-conductivity measurements; the insert shows the points determined by Long *et al.* included in this figure. The logarithmic plot of the quantity $\lambda_g/T^2$ in Fig. 2 reveals a good $T^2$ dependence for temperatures below 1.4°K. This figure also shows a marked rise in conductivity above 1.4°K where, within a range of 2°K, the conductivity rises about 10 times above the expected $T^2$ behavior. The data points of both Long *et al.* and White and Woods are also shown in the figure and seen to blend relatively well with the rest of the data points. Also, there is possibly a slight tendency at the lowest temperature for a departure from the $T^2$ law.

[11] H. M. Rosenberg, Phil. Trans. Roy. Soc. London **247**, 441 (1955).
[12] G. K. White and S. B. Woods, Phil. Mag. **3**, 342 (1958).

*Lattice Conductivity*

A good starting point in interpreting lattice-conductivity data is to refer to Callaway's[13] phenomenological theory in which the relaxation effect from the three-phonon normal process is taken into account. Calling $\tau_N^{-1}$ the relaxation frequency due to the three-phonon normal scattering and $\tau^{-1}$ the combined resistive scattering frequency of phonons by other processes, it is found that the conductivity regime depends greatly on the relative value taken by these frequencies as the conductivity takes the form

$$\lambda_g=\frac{K}{2\pi^2 v_s}\left(\frac{KT}{\hbar}\right)^3\left(A_1+\frac{A_2^2}{A_3}\right), \tag{1}$$

with

$$A_1=\int_0^{\Theta/T}\frac{1}{\tau^{-1}+\tau_N^{-1}}\frac{x^4e^x}{(e^x-1)^2}dx, \tag{2a}$$

$$A_2=\int_0^{\Theta/T}\frac{\tau_N^{-1}}{\tau^{-1}+\tau_N^{-1}}\frac{x^4e^x}{(e^x-1)^2}dx, \tag{2b}$$

$$A_3=\int_0^{\Theta/T}\frac{\tau_N^{-1}\tau^{-1}}{\tau^{-1}+\tau_N^{-1}}\frac{x^4e^x}{(e^x-1)^2}dx. \tag{2c}$$

Isotropy and absence of dispersion in the crystal-vibration spectrum are assumed and no distinction is made between longitudinal and transverse phonons. As implied by these three assumptions, $v_s$ is the velocity of

[13] Joseph Callaway, Phys. Rev. **113**, 1046 (1959); **122**, 787 (1961).

sound.[14–16] The parameter $x=\hbar\omega/KT=\hbar qv_s/KT$, where $\omega$ and $q$ are the phonon frequency and wave vector, respectively. The limit of integration $x_D=\Theta/T$ corresponds to $\omega=\omega_D$ or $q=q_D$ with $\Theta$, $\omega_D$, and $q_D$ the Debye temperature, Debye cutoff frequency, and the radius of the Debye sphere, respectively.

In the integrals (2) the diverse scattering functions are weighted by the term $x^4e^x(e^x-1)^{-2}$. If the condition $\tau_N^{-1}<\tau^{-1}$ prevails in the weighted part of the integrals, it may be seen that $A_2^2/A_3$ may be neglected relative to $A_1$ and the conductivity becomes

$$\lambda_g=\frac{K}{2\pi^2v_s}\left(\frac{KT}{\hbar}\right)^3\int_0^{\Theta/T}(\tau^{-1}+\tau_N^{-1})^{-1}\frac{x^4e^x}{(e^x-1)^2}dx, \quad (3a)$$

and eventually for $\tau_N^{-1}\ll\tau^{-1}$,

$$\lambda_g=\frac{K}{2\pi^2v_s}\left(\frac{KT}{\hbar}\right)^3\int_0^{\Theta/T}\tau\frac{x^4e^x}{(e^x-1)^2}dx. \quad (3b)$$

The condition $\tau_N^{-1}<\tau^{-1}$ is characteristic of a poor phonon mixing.

Under the opposite condition of strong phonon-phonon $N$-process $\tau_N^{-1}>\tau^{-1}$, the conductivity takes the form as obtained by Ziman[4] and by Makinson[2];

$$\lambda_g=\frac{K}{2\pi^2v_s}\left(\frac{KT}{\hbar}\right)^3\mathcal{J}_4^2\left(\frac{\Theta}{T}\right)\Big/\int_0^{\Theta/T}\tau^{-1}\frac{x^4e^x}{(e^x-1)^2}dx, \quad (4)$$

where $\mathcal{J}_4(x_D)$ is the Debye function[17] of order 4.

The choice of the forms (1), (3a), (3b), or (4) to be used to analyze conductivity data depends on the knowledge of the different scattering effects, and the prevalence at a given temperature of one of them in the weighted part of the integrals (2).

*Scattering of the phonons.* The principle of additivity of the resistive scattering relaxation frequencies may be used with

$$\tau^{-1}=\tau_b^{-1}+\tau_c^{-1}+\tau_{iso}^{-1}+\tau_u^{-1}, \quad (5)$$

taking into account the scattering by the boundaries, the charge carriers, the isotopes, and umklapp phonons, respectively, other scattering mechanisms being neglected.

*Phonon-boundary scattering.* The scattering relaxation frequency by crystal boundaries and surface dislocations $\tau_b^{-1}$ is constant; $\tau_b^{-1}=b=v_s/\Lambda$, where $\Lambda$, the Casimir length,[18] is of the order of the crystal size. For a rectangular cross section $\Lambda=1.12l$ with $l$ the mean width of the section. For the crystal under study, $\tau_b^{-1}\simeq0.8\times10^6$ sec$^{-1}$.

*Phonon-electron scattering.* The scattering by the charge carriers is of the form $\tau_c^{-1}=6\tau_h^{-1}+3\tau_e^{-1}$; $\tau_h^{-1}$ is the scattering relaxation frequency due to the hole carriers contained in one of the hole Fermi pockets and $\tau_e^{-1}$ corresponds to that of an electron pocket. There are six hole pockets and three electron pockets in antimony which contribute independently to the scattering as long as the $q$'s are small enough not to scatter carriers from one pocket to another.

The $\tau_h^{-1}$ and the $\tau_e^{-1}$ can be approximately formulated if besides the phonon-isotropy assumption, the carrier pockets are supposed to be isotropic (spherical) and to obey a quadratic energy law; then[19]

$$\tau_h^{-1}(q)\simeq\frac{m_h^2\mathcal{E}_{def}^2}{2\pi\rho h^3}q, \quad \text{for } q\leq2k_h$$

and

$$\tau_h^{-1}(q)=0, \quad \text{for } q>2k_h \quad (6)$$

with similar equations for $\tau_e^{-1}$.

The effective masses of the carrier are $m_h$ and $m_e$; the deformation potential $\mathcal{E}_{def}$ will be supposed the same in absolute values for both bands, $\rho$ is the mass density and the radii $k_F$ of the Fermi pockets are respectively $k_h$ and $k_e$. Under the assumption of isotropic and quadratic Fermi pockets, masses and radii can be approximated[20–23] with $k_e\simeq8.1\times10^6$ cm$^{-1}$, $k_h\simeq6.4\times10^6$ cm$^{-1}$, $m_e\simeq0.28m_0$, and $m_h\simeq0.14m_0$.

---

[14] The sound velocity average $v_s$ will be taken as $2.5\times10^5$ cm/sec in most calculations. As shown by the room-temperature data of Epstein and DeBretteville (Ref. 15), the velocity is highly anisotropic, with longitudinal velocities from 4.19 to $2.59\times10^5$ cm/sec and transverse velocities from 2.93 to $1.51\times10^5$ cm/sec, depending on the propagation direction. Even though the different averages $(\langle v^n\rangle\langle v^p\rangle)^{1/(n+p)}$ should depend strongly on $n$ and $p$, no attempt was made to obtain those averages. (See Ref. 16.) The Debye velocity $v_D=K\Theta/\hbar(6\pi^2N)^{1/3}$ is equal to approximately $2.2\times10^5$ cm/sec for $\Theta=210$°K.

[15] S. Epstein and A. P. DeBretteville, Jr., Phys. Rev. **138**, A771 (1965); DeBretteville *et al.*, *ibid.* **148**, 575 (1966).

[16] W. V. Houston, Rev. Mod. Phys. **20**, 161 (1948); D. D. Betts, A. B. Bhatia, and G. K. Horton, Phys. Rev. **104**, 43 (1956).

[17] Debye integrals are of the form

$$\mathcal{J}_n(x_D)=\int_0^{x_D}\frac{x^ne^x}{(e^x-1)^2}dx,$$

with $\mathcal{J}_n(x_D)\simeq(n-1)^{-1}x_D^{n-1}$ for $x_D\to0$ and $\mathcal{J}_n(x_D)\simeq n!\zeta(n)$ as $x_D\to\infty$. The Riemann zeta function $\zeta(n)$ takes, for example, the values $\zeta(3)=1.202$, $\zeta(4)=1.082$, $\zeta(5)=1.037$, and $\zeta(8)=1.004$.

[18] H. B. G. Casimir, Physica **5**, 495 (1938).

[19] A. Sommerfeld and H. Bethe, in *Hanbuch der Physik* edited by H. Geiger and K. Scheel (Julius Springer, Berlin, 1933), Vol. 24/2, p. 333; see also Ref. 28, p. 77 and Ref. 3, p. 330.

[20] Under isotropic- and quadratic-energy distribution, the Fermi pockets of holes and electrons are spheres of radius $k_e$ and $k_h$ given by $k_e=(3\pi^2\frac{1}{3}n)^{1/3}$ and $k_h=(3\pi^2\frac{1}{6}n)^{1/3}$. The isotropic effective mass is given by $m_e=\hbar^2k_e^2/2\mu_e$, the density of states by $Z_e=3n/2\mu_e$, the scattering effective Debye temperature by $\Theta_e=\hbar v_s2k_e/K$, and similar expressions for the holes. In agreement with Windmiller (Ref. 21) and Brandt *et al.* (Ref. 22), the number of carriers per band is taken equal to $n=5.45\times10^{19}$ cm$^{-3}$. The chemical potential under the assumption of a parabolic distribution is taken as $\mu_e=14.1\times10^{-14}$ erg and $\mu_h=18.2\times10^{-14}$ erg, an average between the values given by Brandt (Ref. 22) and Rao (Ref. 23). With these values and with $v_x=2.5\times10^5$ cm/sec, the different electronic parameters are $k_h=6.4_3\times10^6$ cm$^{-1}$, $k_e=8.1_1\times10^6$ cm$^{-1}$; $m_h\simeq0.13_8m_0$, $m_e\simeq0.28_4m_0$; $\Theta_h^*\simeq24.4$°K, $\Theta_e^*\simeq30.8$°K; $Z_h=0.45\times10^{33}$ erg$^{-1}$ cm$^{-3}$, $Z_e=0.58\times10^{33}$ erg$^{-1}$ cm$^{-3}$.

[21] L. R. Windmiller, Phys. Rev. **149**, 472 (1966).

[22] N. B. Brandt, N. Ya. Minina, and Chu Chen-Kang, Zh. Eksperim. i Teor. Fiz. **51**, 108 (1966) [English transl.: Soviet Phys.—JETP **24**, 73 (1967)].

[23] G. N. Rao, N. H. Zebouni, C. G. Grenier, and J. M. Reynolds, Phys. Rev. **133**, A141 (1964).

The selective scattering as described in Eq. (6) is due to the normal-scattering momentum-conservation requirement

$$\mathbf{q}=\mathbf{k}'-\mathbf{k}, \quad |\mathbf{k}'-\mathbf{k}|\leq 2k_{\mathrm{F}},$$

and in the conductivity integrals it would correspond to breaking the range of integration into three ranges: (a) $0<q<2k_{\mathrm{h}}$ or $0<x<\Theta_{\mathrm{h}}^*/T$, where $\tau^{-1}=\tau'^{-1}+cxT$, with

$$c=\frac{(6m_{\mathrm{h}}^2+3m_e^2)K}{2\pi\rho v_s\hbar^4}\mathcal{E}_{\mathrm{def}}^2; \tag{7}$$

(b) $2k_{\mathrm{h}}<q<2k_e$ or $\Theta_{\mathrm{h}}^*/T<x<\Theta_e^*/T$, where $\tau^{-1}=\tau'^{-1}+c'xT$, with

$$c'=\frac{3m_e^2K}{2\pi\rho v_s\hbar^4}\mathcal{E}_{\mathrm{def}}^2;$$

(c) $2k_e<q<q_D$ or $\Theta_e^*/T<x<\Theta/T$, where $\tau^{-1}=\tau'^{-1}$. In the three cases above, $\tau'^{-1}$ represents the scattering other than the carrier scattering.

The effective Debye temperatures $\Theta_{\mathrm{h}}^*$, $\Theta_e^*$, associated with scattering[1,24] are given by

$$\Theta_{\mathrm{h}}^*=(2k_{\mathrm{h}}/q_D)\Theta \text{ or } K\Theta_{\mathrm{h}}^*=\hbar v_s(2k_{\mathrm{h}}), \tag{8}$$

with the same expression for $\Theta_e^*$. With the isotropic assumption,[20] one finds $\Theta_{\mathrm{h}}^*\simeq 24.4°\mathrm{K}$ and $\Theta_e^*\simeq 30.8°\mathrm{K}$.

The first range of integration accounts for the phonons scattered by both holes and electrons. In the second range the phonons are still scattered by the electrons, whereas the third range accounts for the phonons which are scattered by neither of the carriers. Those phonons which are outside the sphere of diameter $2k_e$ will be referred to as the "peripheral" phonons.

It may be noted that the anisotropy in $k_{\mathrm{h}}$ and $v_s$ would lead Eq. (8) to determine a whole spectrum of $\Theta^*$ values and widen the range of temperatures in which the peripheral phonons become efficient. The effect due to the anisotropy would probably be more important than the effect brought about by the distinction between holes and electrons. In view of this, the data will be analyzed by considering a single empirical $\Theta^*$ to be determined from experimental data.

Should it be recognized that the regime of conductivity is such as to be given by formula (3a) or (3b), the expression to be analyzed will be

$$\lambda_g=\frac{K}{2\pi^2v_s}\left(\frac{KT}{\hbar}\right)^3\left\{\int_0^{\Theta^*/T}(\tau'^{-1}+cxT)^{-1}\frac{x^4e^x}{(e^x-1)^2}dx+\int_{\Theta^*/T}^{\Theta/T}\tau'\frac{x^4e^x}{(e^x-1)^2}dx\right\}. \tag{9}$$

*Phonon-isotope scattering.* The relaxation frequency associated with isotope scattering[25,26] is given in the nondispersive case by

$$\tau_{\mathrm{iso}}^{-1}=Dq^4=dx^4T^4, \tag{10}$$

where $D=v_s\sum_i N_i\langle\delta M_i\rangle^2/4\pi\rho^2$ and $d=DK/\hbar v_s$. $N_i$ is the number of a given kind of isotope atoms (per cm$^3$); $\langle\delta M_i\rangle^2=(M_i-\bar{M})^2$, with $M_i$ the isotope mass and $\bar{M}$ the average atomic mass. The above expression in the case of natural antimony gives $D\simeq 4\times10^{-23}$ cm$^{-4}$ sec$^{-1}$ and $d\simeq 3.07°\mathrm{K}^{-4}$ sec$^{-1}$.

*Phonon-phonon scattering.* The normal three-phonon relaxation frequency as used by Callaway[13] is given by Herring[27] as

$$\tau_N^{-1}\propto x^pT^5 \quad \text{or} \quad \tau_N^{-1}\propto q^pT^{5-p},$$

with $p=2$ in cubic symmetry and $p=3$ in an anisotropic structure for the nondispersive longitudinal phonons.

The umklapp process[27] leads to scattering of the form

$$\tau_{\mathrm{u}}^{-1}=f(T,q)e^{-\Theta/\alpha T}, \tag{11}$$

where $\alpha$ is usually expected in the range $1<\alpha<2$. The form of $f(T,q)$ is still a matter of much conjecture. Thus $f(T,q)$ could be taken proportional to $qT^{-1}$,[28] $q^2T^3$,[13] or $q^2T$.[29] More complex forms for $\tau_{\mathrm{u}}^{-1}$ could also be used.[29] The form given by Klemens,[28]

$$\tau_{\mathrm{u}}^{-1}\simeq 8\Gamma^2(K\Theta/Mv_s)bxe^{-\Theta/\alpha T}, \tag{12}$$

is numerically calculable, with $\Gamma$ the Grüneisen constant and $b$ the reciprocal lattice vector which in the cubic case can be approximated by $2\pi(V_a)^{-1/3}$, where $V_a$ is the atomic volume.

The total phonon scattering may take the form

$$\tau^{-1}\simeq b+cxT+dx^4T^4+uxe^{-\Theta/\alpha T} \tag{13a}$$

and

$$\tau_N^{-1}\sim x^2T^5, \tag{13b}$$

and it may be seen from the temperature dependence that if $b$, $c$, $d$, and $u$ are properly chosen, the preponderant scattering may be as given above, i.e., near zero temperature boundary scattering is preponderant, then electron scattering and the isotope effect, and finally umklapp processes for higher temperatures. The normal process, depending on the case, may become important at any point in the sequence above. Only the order of magnitudes in particular cases will determine this point. That is to say, the data at a given temperature may be approached *a priori* and in the first-order approximation either by use of the weak mixing formula (3b) or the strong-mixing Ziman formula (4) until the proper magnitude of $\tau_N^{-1}$ has been established.

In the first attempt to analyze their data in the range 1.5–4.2°K, Long *et al.*[1] noted that there was an apparent agreement between the ratio $\lambda_g/\sigma_i$ of lattice conductivity to ideal electrical conductivity and the formula obtained for this ratio by Ziman[4] in the strong-

[24] E. H. Sondheimer, Proc. Phys. Soc. (London) **A65**, 561 (1952).
[25] Peter Carruthers, Rev. Mod. Phys. **33**, 92 (1961).
[26] P. G. Klemens, Proc. Phys. Soc. (London) **A68**, 1113 (1955).
[27] Conyers Herring, Phys. Rev. **95**, 954 (1954).
[28] P. G. Klemens, in *Solid State Physics*, edited by F. Seitz and D. Turnbull (Academic Press Inc., New York, 1958), Vol. 7, p. 87.
[29] Philip D. Thacher, Phys. Rev. **156**, 975 (1967).

mixing limit and the case of phonon-electron preponderant scattering, i.e.,

$$\frac{\lambda_g}{\sigma_i}=\left(\frac{K}{e}\right)^2\frac{T}{n_a^2}\left(\frac{C_g}{3NK}\right)^2, \tag{14}$$

where $n_a$ is the number of electrons per atom in a corresponding single-band model and $C_g$ is the lattice specific heat

$$C_g=9NK(T/\Theta)^3\mathcal{J}_4(\Theta/T), \tag{15a}$$

which at low temperature tends to

$$C_g=233.7NK(T/\Theta)^3. \tag{15b}$$

This agreement prompted them to analyze $\lambda_g$ on the Ziman form of Eq. (4) which could be rewritten using Eq. (7) in the case of preponderant electron scattering as

$$\lambda_g=\frac{K}{2\pi^2v_s}\left(\frac{KT}{\hbar}\right)^3\mathcal{J}_4^2(\infty)\left[cT\mathcal{J}_5\left(\frac{\Theta^*}{T}\right)+\text{negligible terms}\right]^{-1}, \tag{16}$$

which, with the values of $c\simeq 15.5\times10^6$ (sec °K)$^{-1}$ and $\Theta^*\simeq 11$°K, was found to agree well with the experimental data.

The extension of the thermal-conductivity measurements to lower temperatures[30] shows the expected appearance of the $T^2$ behavior of $\lambda_g$ as $\Theta^*/T\to\infty$, but the value of $\lambda_g$ is about 30% above what is expected from the extrapolation of Eq. (16). It is then interesting and tempting to note that the discrepancy can be practically compensated by replacing in Eq. (16) the quantity $\mathcal{J}_4^2(\infty)\mathcal{J}_5^{-1}(\infty)$ by $\mathcal{J}_3(\infty)$ which amounts to a shift from the strong- to the weak-mixing formula (18) extended to low temperature. This would suggest that the three-phonon process scattering frequency $\tau_N^{-1}$, while negligible below 1.5°K, would become dominant above this temperature.

Despite this apparent agreement, the above conclusion is strongly in doubt since this would call for a value of $\Theta^*$ too small compared to the expected value and, more important, call for a value of $\tau_N^{-1}$ far above expectation. The value $\tau_N^{-1}\simeq 10^8$ sec$^{-1}$ which is implied for $T\simeq 1.5$°K is only to be expected near $T\simeq 10$°K. The apparent agreement with Ziman's $\lambda_g/\sigma_i$ value of Eq. (14) may be purely accidental and should not be taken too seriously.

Thus an attempt should be made then to interpret the data in the form of the weak-mixing formulas (3b) and (9) all through the helium-temperature range.

Below 1.4°K the near $T^2$ dependence of $\lambda_g$ strongly suggests that in the first term in Eq. (9) the electron scattering is preponderant and that the second term in Eq. (9) is negligible, so that $\lambda_g$ can be approximated in this range (with $\Theta^*/T\to\infty$) by

$$\lambda_g\simeq\frac{K}{2\pi^2v_s}\left(\frac{KT}{\hbar}\right)^3\int_0^\infty\frac{1}{b+cxT}\frac{x^4e^x}{(e^x-1)^2}dx, \tag{17}$$

with $b=0.8\times10^6$ sec$^{-1}$ and $c=14.5\times10^6$(°K sec)$^{-1}$ and is represented below 1.4°K by the continuous line in Fig. 2 (where the associated quantity $\lambda_gT^{-2}$ is plotted).

This first term at higher temperature would tend toward

$$\frac{K}{2\pi^2v_s}\left(\frac{KT}{\hbar}\right)^3\frac{1}{cT}\mathcal{J}_3\left(\frac{\Theta^*}{T}\right) \tag{18}$$

as the effect of $b$ is becoming negligible and the isotope effect is still negligible. This term is outlined above 1.4°K by the dashed lines in Fig. 2 for three different values of $\Theta^*$ and seen to decrease below the $T^2$ behavior.

Above 1.4°K the sharp increase in conductivity will be associated with the second term in Eq. (9) which represents the contribution of the peripheral phonons

$$\Delta\lambda_g\simeq\frac{K}{2\pi^2v_s}\left(\frac{KT}{\hbar}\right)^3\int_{\Theta^*/T}^\infty\frac{1}{(b+dT^4x^4)}\frac{x^4e^x}{(e^x-1)^2}dx \tag{19}$$

as $\Theta/T$ is taken as $\infty$. The global result obtained for $\lambda_g$ counting the two terms (18) and (19) with $b=0.8\times10^6$ sec$^{-1}$, $d=3.07$°K$^{-4}$ sec$^{-1}$, and $c=14.5\times10^6$(°K sec)$^{-1}$ is shown in Fig. 2 for three values of $\Theta^*$, $\Theta^*=20$, 25, and 30°K, by full lines which are seen to delimit relatively well the region spanned by the experimental points. An almost good fit is obtained for $\Theta^*=25$°K, i.e., close to the value calculated for $\Theta_h^*$.

The fact that the experimental points seem to span a spectrum of values of $\Theta^*$ ranging from about 20 to 30°K is in agreement with the qualitative considerations made previously on the anisotropy of the pockets and the existence of two bands of charge carriers.

Although one could consider that the experimental points are falling behind the steep rise of the theoretical curves because of the added scattering represented by the increase of $\tau_N^{-1}$ with temperature, this increase is probably still insufficient at these temperatures to account for the observed values. The results are therefore seen to be in agreement with the right order of magnitude for $\tau_B^{-1}$, $\tau_{iso}^{-1}$, and $\Theta^*$ but cannot be used for precise measurement of these quantities; nor can it be used to map the peripheral phonons.

Note that there is an apparent discrepancy with the conclusion of White and Woods about the importance of the isotope effect. But it seems more likely in this case that their conclusion sprang from a numerical error, and it would be interesting to see if their data could not be reinterpreted with the isotope effect included. If it is supposed that $\tau_N^{-1}$ is dominant above 20°K, the strong-mixing formula of Makinson-Ziman[4]

[30] R. S. Blewer and N. H. Zebouni, Phys. Letters 23, 297 (1966).

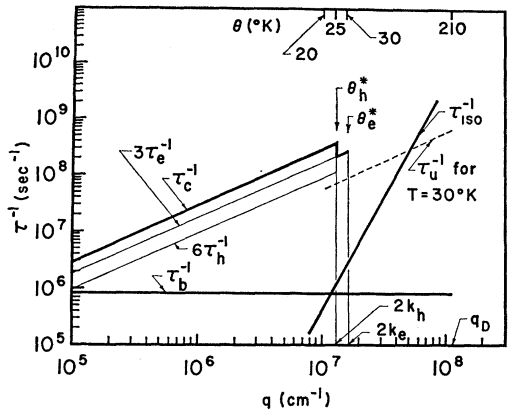


FIG. 3. The relaxation frequencies of the phonons for different scattering mechanisms versus the phonon wave vector $\mathbf{q}$. The boundary contribution $\tau_b^{-1}\simeq 0.8\times 10^6$ sec$^{-1}$ and the isotope contribution $\tau_{iso}^{-1}\simeq 4\times 10^{-23}q^4$ sec$^{-1}$ are calculated. The electron-phonon scattering frequency $\tau_c^{-1}=27.5q$ sec$^{-1}$ ($q$ in cm$^{-1}$) is obtained from the experimental data. The separate scattering contributions of holes and electrons are sketched, and are seen to occur only for $q<2k_e$, $2k_h$. The sharp decrease of the scattering at $q=2k_e$, $2k_h$ reflects the behavior of peripheral phonons whose contribution to the conductivity is shown in Fig. 4. The umklapp scattering frequency $\tau_u^{-1}$ is shown for $T=30$°K by the dashed line.

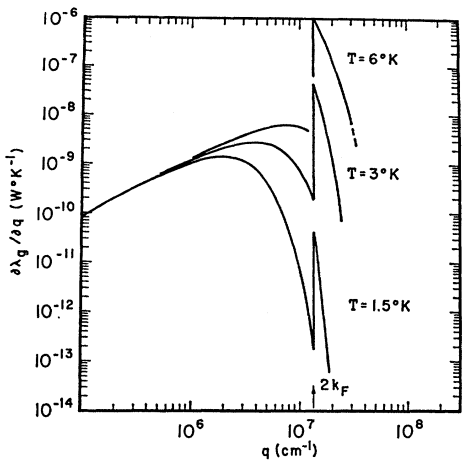


FIG. 4. Contribution of the phonons to the lattice conductivity as a function of their $q$ value at different temperatures. The quantity

$$\partial\lambda_q\frac{\partial\lambda_q(q)}{\partial q}=\frac{K}{2\pi^2}\left(\frac{KT}{\hbar}\right)^2\tau\frac{x^4e^x}{(e^x-1)^2}$$

represents in the low-temperature limit the contribution to the lattice conductivity of the different phonons as a function of the magnitude of their wave vector $q=(KT/\hbar v_s)x$. The relaxation time $\tau$ is given through Eq. (7) in which it has been assumed that $\Theta^*=\Theta_h^*=\Theta_e^*=25$°K or $k_F=k_h=k_e$. The peripheral phonons ($q>2k_F$) are seen to exhibit a sharp contribution, negligible at $T=1.5$°K, preponderant at $T=3$°K and above.

may be used between 20 and 100°K, with

$$\tau^{-1}=\tau_c^{-1}+dx^4T^4+uxe^{-\Theta/\alpha T} \tag{20a}$$

or

$$\lambda_q=\left[\frac{K}{2\pi^2v_s}\left(\frac{KT}{\hbar}\right)^3\mathcal{J}_4^2\left(\frac{\Theta}{T}\right)\right]\left[cT\mathcal{J}_5\left(\frac{\Theta^*}{T}\right)+dT^4\mathcal{J}_8\left(\frac{\Theta}{T}\right)+ue^{-\Theta/\alpha T}\mathcal{J}_5\left(\frac{\Theta}{T}\right)\right]^{-1}. \tag{20b}$$

The calculated contribution of the carrier scattering is found to be negligible and, fitting White and Wood's data to Eqs. (20), gives $d\simeq 2.8_5$(°K)$^{-4}$ sec$^{-1}$, $u\approx 1.7\times 10^8$ sec$^{-1}$ and $\alpha\approx 1.35$.

The fact that $d$ differs by less than 10% from the calculated value $d\simeq 3.07$(°K)$^{-4}$ sec$^{-1}$ is well within the range due to errors and the rough approximations made. The umklapp term $u=8\Gamma^2K\Theta b(Mv_s)^{-1}$ determined above corresponds to $\Gamma\approx 1.06$, in good agreement with $\Gamma\approx 0.9$, the room-temperature Grüneisen coefficient as determined from the compressibility, dilation, and specific heat.[31] The value of $\alpha$ is in the acceptable range.

*Deformation potential.* If the value $c=14.5\times 10^6$ (°K sec)$^{-1}$ experimentally determined for the electron-scattering term is used for the calculation of the deformation potential $\mathcal{E}_{def}$ through Eq. (7), the value

$$|\mathcal{E}_{def}|\simeq 1.8\text{ eV}$$

is obtained which is in general agreement with the results on some semiconductors doped to an equivalent carrier density.[32,33] This potential measures the strength of the electron-phonon interaction and would be differently interpreted in the extreme cases of good metals and semiconductors. Thus, due to strong screening in good metals, the dominant term in $\mathcal{E}_{def}$ is given as $\frac{2}{3}E_F$ (where $E_F$ is the Fermi energy). If this result is extrapolated to the case of semimetals, the value obtained should be close to $\frac{2}{3}\mu$, where $\mu$ is the chemical potential, but the term dominant in nonscreened semiconductors would be identified more closely with $\frac{2}{3}E_I$ or $\frac{2}{3}E_A$, where $E_I$ is the ionization energy and $E_A$ is the affinity potential. The semimetals may appear as intermediate between these limits. Relations such as

$$\mathcal{E}_{def}(\text{holes})=-\mathcal{E}_{def}(\text{el}) \tag{21}$$

and

$$|\mathcal{E}_{def}(\text{holes})|+|\mathcal{E}_{def}(\text{el})|=|\partial\mathcal{E}_{gap}/\partial\Delta| \tag{22}$$

are expected to hold.[34] The first relation has been assumed in writing Eq. (7) and may help to estimate the contribution of each band to the scattering of the phonons which is then roughly found to be 67% due to the electrons and 33% due to the holes. These separate relaxation frequencies are displayed in Fig. 3 as a function of $q$ together with the combined frequency $\tau_c^{-1}$. The second relation indicates that $|\partial\mathcal{E}_{gap}/\partial\Delta|\simeq 3.6$ eV.

[31] $\Gamma=3\alpha BC_v^{-1}$, with room-temperature data for compressibility (Ref. 15) $B=3.86\times 10^{11}$ dyn cm$^{-2}$, for specific heat $C_v=1.4\times 10^{-7}$ erg cm$^{-3}$ and linear dilation coefficient $\alpha=10.8\times 10^{-6}$ (°K)$^{-1}$. $C_v$ and $\alpha$ taken from *Handbook of Chemistry and Physics* (The Chemical Rubber Publishing Co., Cleveland, Ohio), 44th ed.

[32] M. G. Holland, Phys. Rev. 134, A471 (1964).

[33] E. F. Steigmeier and B. Abeles, in *Proceedings of the Seventh International Conference on the Physics of Semiconductors Paris, 1964*, (Academic Press Inc., New York, 1965), p. 701.

[34] Reference 3, p. 205.

*Peripheral phonons.* To summarize, the different scattering relaxation frequencies are shown in Fig. 3 as a function of $q$. Here $\tau_b^{-1}$ and $\tau_{iso}^{-1}$ are obtained from theoretical consideration, $\tau_c^{-1}$ from experimental determination. It clearly appears that the band of peripheral phonons ($q>2k_e$) around $q\approx 1.5\times 10^7$ cm$^{-1}$, nonscattered by the electrons, has a relaxation frequency one or two orders of magnitude smaller than other neighboring phonons and should, at certain temperatures, greatly influence the conductivity.

This point is better emphasized in Fig. 4, where the quantity

$$\frac{\partial\lambda_g(q)}{\partial q}=\frac{K}{2\pi^2}\left(\frac{KT}{\hbar}\right)^2\tau(x,T)\frac{x^4e^x}{(e^x-1)^2} \tag{23}$$

is displayed versus $q=(KT/\hbar v_s)x$. This quantity corresponds to the term integrated in Eq. (3b) and represents the contribution to the lattice conductivity of the different phonons as a function of the magnitude of their wave vector. The three curves correspond to $\Theta^*=25$°K and describe the term (23) for the three different temperatures $T=1.5$, 3, and 6°K. Each exhibits the sharp-peaked contribution of the peripheral phonons above $q=2k_F$ and it may be seen that this contribution changes from negligible at 1.5°K to preponderant at $T=3$°K and above. The resulting effect on $\lambda_g$ is shown in Fig. 2.

### B. NE Effect at High Field, Electronic and Phonon Drag Contributions, and Electronic Density of States

The density of electronic states at the Fermi surface is related to the components of the kinetic thermoelectric tensor $\boldsymbol{\varepsilon}''$, where $\boldsymbol{\varepsilon}''$ is defined through the kinetic equation

$$\mathbf{J}=\boldsymbol{\sigma}\cdot\mathbf{E}^*+\boldsymbol{\varepsilon}''\cdot\boldsymbol{\nabla}T, \tag{24}$$

with $\mathbf{J}$ the current density, $-\mathbf{E}^*$ and $\boldsymbol{\nabla}T$ the gradient of electrochemical potential and of temperature, respectively, $\boldsymbol{\sigma}$ and $\boldsymbol{\varepsilon}''$ the conductivity and thermoelectric tensors, respectively. The density of states would generally appear in $\boldsymbol{\varepsilon}''$ as an average with the mobility over bands and possibly states.

Great simplifications occur at high field in the case of a Fermi surface with closed orbits, both in the theoretical expression for $\boldsymbol{\varepsilon}''$ and in its experimental determination.

The classical mobility of every carrier is known to tend at high field toward the common limit $ic/H$, the Hall mobility. Therefore Eq. (24) takes the simple form

$$J_x=(c/H)F_y, \tag{25}$$

where $F_y$ is the effective driving force acting on the electron system, with

$$F_y=(n_h-n_e)eE_y+\nabla_y\{P_{el}+rP_g\}; \tag{26}$$

$E$ is the electrostatic field, $P_{el}$ and $P_g$ are the "pressures" of the electron and phonon gases, respectively; $r$ indicates the fraction of momentum of the phonon system transferred to the electron system, and $n$ is the density of carriers. Lorentz forces are excluded from Eq. (26) and the umklapp effect is neglected.

The notion of electron gas pressure is valid in the classic case of a quadratic-distribution function for which $P_x=n\langle k_x\partial\mathcal{E}/\partial k_x\rangle$ is independent of the $x$ direction. At high field, with more complex surfaces the pressure can be anisotropic and, in this case, the components perpendicular to the field can be taken[35] as $P_\perp=n\langle\mathcal{E}_\perp\rangle$. For $\mathcal{E}_\perp=\omega_c(p+\frac{1}{2})$, isotropy of $P$ in the plane perpendicular to the field ensues, but generally $P_\perp\neq P_{||}$ and will remain different in the classical limit too. It is not expected, either, that the phonon pressure should be isotropic.

Under the simplifying assumption of isotropic pressures, the pressure $P=\Omega$ (the grand canonical potential per unit volume) and Eq. (25) becomes

$$J_x=\frac{c}{H}\left[(n_h-n_e)eE_y+\frac{\partial\Omega_{el}}{\partial\mu}\nabla_y\mu+\frac{\partial(\Omega_{el}+r\Omega_g)}{\partial T}\nabla_yT\right]$$

or

$$J_x=(n_h-n_e)\frac{ec}{H}E^*_y-\frac{c}{H}(s_{el}+rs_g)\nabla_yT. \tag{27}$$

The temperature dependence of $r$ has been neglected for simplification. In the low-temperature limit with the electron entropy density $s_{el}=C_{el}=\frac{1}{3}\pi^2K^2TZ$ and in the low-temperature Debye approximation for which the phonon entropy $s_g=\frac{1}{3}C_g=\frac{1}{3}(12\pi^2\frac{1}{5}NK)(T/\Theta)^3$, the NE kinetic coefficient takes the value

$$\epsilon_{12}''=-(c/H)(C_{el}+\tfrac{1}{3}rC_g) \tag{28a}$$

or

$$\epsilon_{12}''=-\frac{\pi^2K^2cT}{3H}\left[Z+r\frac{12\pi^2}{5}\frac{N}{K\Theta}\left(\frac{T}{\Theta}\right)^2\right], \tag{28b}$$

and this coefficient is seen to measure not only the electronic specific heat, but also $\frac{1}{3}$ of the specific heat of the fraction of phonons dragged by the electrons.

Besides this greatly simplified expression for $\epsilon_{12}''$, the experimental determination of this coefficient is also simplified. At high field it is expected and found that $\sigma_{12}/\sigma_{11}$ and $\lambda_{12}/\lambda_{11}$ become negligible as well as the correction for the thermocouple effect of the leads and the coefficient $\epsilon_{12}''$ is well approximated by the expression $\epsilon_{12}''=\epsilon_{12}'/\rho_{11}\gamma_{11}$, all these coefficients being directly measured experimentally. ($\epsilon_{12}'=-E_y/w_x^*$ for $J=0$, $w_x^*$ is the heat flow density, and $\rho_{11}$ and $\gamma_{11}$ are the electronic and thermal magnetoresistivities, respectively.)

*Electronic density of states.* The total density of electronic states at the Fermi surface $Z$ would be directly measured by the apparent quantity $Z^{eff}=-3H\epsilon_{12}''/$

[35] V. G. Bar'Yakhtar and S. V. Peletminskii, Zh. Eksperim. i Teor. Fiz. 48, 187 (1965) [English transl.: Soviet Phys.—JETP 21, 126 (1965)].

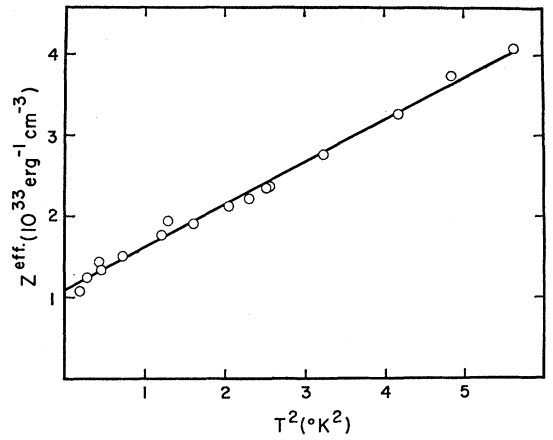


FIG. 5. The apparent density of electronic states at the Fermi surface of Sb, $Z^{eff}$ determined from the high-field limit of the NE thermoelectric coefficient versus $T^2$. The extrapolation to $T^2=0$ gives the electronic density of states $Z$. The additional contribution due to phonon drag appears as the term proportional to $T^2$.

$\pi^2K^2cT$ should the drag term be negligible. But, as shown in Fig. 5, this quantity is found to be temperature-dependent with (to a good approximation) the expected $T^2$ dependence of an added drag term. The extrapolation of $Z^{eff}$ to $T=0$ gives the electronic part $Z=(1.10\pm0.07)$ $10^{33}$ erg$^{-1}$ cm$^{-3}$, and the $T^2$-dependent part yields the value $50.4\pm1.2$ in J deg$^{-4}$ mole$^{-1}$ for the quantity $\frac{1}{3}rC_gT^{-3}$. The results are in gross agreement with the rough determination of Long *et al.*[1] using also the NE determination. The electronic part is also in fair agreement with the value obtained from[20] $Z=\sum\frac{3}{2}n_i/\mu_i$ in the quadratic-distribution approximation with $Z=1.03\times10^{33}$ erg$^{-1}$ cm$^{-3}$.

Comparison of the NE density-of-states determination with the determination through the specific heat is shown in Table I. It may be seen that the NE density of states is generally larger than the specific-heat determination by 10–20% depending on the reference. It is believed that experimental error would not account for all the discrepancy. Most probably a departure from quadratic distribution in antimony is the cause of this discrepancy, with $\mathrm{grad}n\langle\mathcal{E}_\perp\rangle\neq\frac{2}{3}\,\mathrm{grad}n\langle\mathcal{E}\rangle$, the first quantity being 1.1–1.20 times smaller than the second.

The question of comparing bare electrons (b.e.) with quasiparticle (q.p.) electrons could be raised at this point with the NE for measurement of the former[36] and specific heat defining the latter. The ratio in masses of the two kinds of electrons would be in direct ratio with the density of states they depend upon, $m_{b.e.}/m_{q.p.}=Z_{NE}/Z_{Sp.H.}$. This ratio should be smaller than unity to account for the quasiparticle added mass but is found from measurements to be larger than unity. This should not be taken as a contradiction because the effect of the nonquadratic anisotropic energy distribution is most probably preponderant over the quasiparticle added mass effect.

[36] R. E. Prange and L. P. Kadanoff, Phys. Rev. 134, A566 (1964).

TABLE I. Data on specific-heat and transport effects. $C/T=\alpha T^{-3}+\beta T^2+\gamma$ in $10^{-6}$ J deg$^{-2}$ mole$^{-1}$ ($T$ in °K). In the present work, errors are determined taking 95% confidence limits and error is taken to be 1.965 times the first standard deviation. The coefficients were obtained from the data by fitting the previous equation using a multiple regression program of General Foods.

| | Transp. effects | Specific heat | | |
|---|---|---|---|---|
| | This work | This work | Ref. 38 | Ref. 40 |
| Temp. range (°K) | 0.4–2.3 | 0.37–1.4 | 0.54–1.1 | 0.5–4.0 |
| $\alpha$ | ··· | 1.97±0.23 | 4.8±0.4 | ··· |
| $\beta$ | 186±6[a] | 211±5.3 | 210±2 | 206±1 |
| $\gamma$ | 127±7 | 116.5±6.4 | 105±2 | 112±5 |
| $\Theta$(°K) | 218[a]±2 | 209.6±1.18 | 210±0.7 | 211.3±1.5 |
| $Z\left(\frac{10^{33}}{\text{erg cm}^3}\right)$ | 1.10±0.07 | 1.01±0.05 | 0.916 | 0.97 |

[a] $C_gT^{-1}=\beta T^2$ and $\Theta$ are obtained from Eq. (28a) and Fig. 6, lower curve, by assuming a (97.5±1.5)% phonon drag for calculating $C_g$.

*Phonon drag.* Below 1.4°K, where the effect of the peripheral phonons is negligible, phonons will be mainly scattered by the electrons and, to a lesser extent, by the boundaries. It may be estimated that boundaries contribute to approximately 1–4% of the total scattering in the range 0.5–1.4°K. This will make the drag efficiency $r\approx96$–$99\%$, which, when used in conjunction with the drag term in Eqs. (28) and its experimentally determined value, will give for the lattice specific heat a value $C_g=\beta T^3$, where $\beta=186\pm6$ $\mu$J deg$^{-4}$ mole$^{-1}$ and with an apparent value for the Debye temperature $\Theta=218\pm2$°K. It may be seen in Table I that the NE drag determination of $C_g$ is about 12% smaller than the direct specific-heat determination. Again, in similarity to the case of the electrons, the isotropic distribution of the phonons is far from being achieved and the notion of phonon pressure is only to be taken as a first-order approximation. With $\mathrm{grad}P_{g\perp}\neq\mathrm{grad}P_{g\parallel}$ the apparent directional lattice specific heat measured by the NE effect would be different from the averaging obtained from a specific-heat measurement.

Above 1.4°K a selective drag should appear. Since part of the phonons, i.e., the peripheral phonons, do not scatter the electrons, they are not being dragged either. This is equivalent to replacing in Eq. (28a) $C_g$ by $C_g^*=C_g\mathcal{J}_4(\Theta^*/T)/\mathcal{J}_4(\Theta/T)$, the subthermal phonon specific heat. The decrease in the drag in the temperature range studied due to this effect is still too small for any conclusive evidence of this effect. Note that the temperature dependence of Long's[1] $Z^{eff}$ data may be an indication of it.

In conclusion, the NE measurement leads to a determination of the electron density of states slightly different than its determination from the specific heat. This difference is believed to be associated with the anisotropic nonquadratic electron distribution in antimony. The phonon-drag term also does not match the prescribed lattice specific-heat contribution exactly.

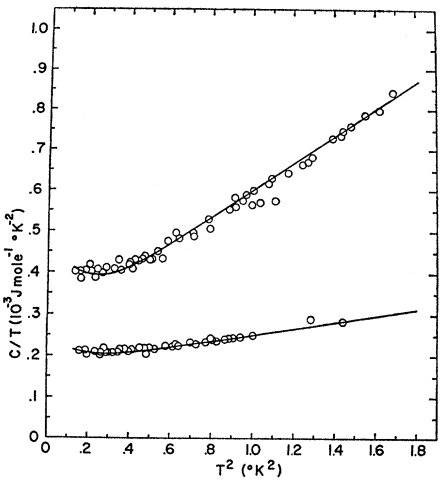


FIG. 6. Specific-heat data for Sb. The upper set of points are experimental results for sample plus addenda. The lower set of points are the data for specific heat of the addenda. The solid lines represent least-square fits to Eq. (32).

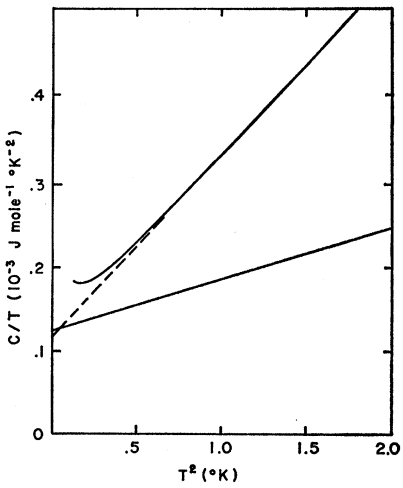


FIG. 7. Comparison of specific-heat and thermoelectric results expressed in units of $C/T$ versus $T^2$. The upper curve is derived from the specific-heat results: The slope of the dashed straight line is a measure of the Debye temperature $\Theta$; its intercept is a measure of the electronic specific-heat coefficient $\gamma$; influence of the nuclear-quadrupole contribution is evident at the lowest temperatures. The lower curve represents the thermoelectric data in the same units.

This is probably a consequence of the anisotropic phonon distribution.

### C. Specific Heat

In addition to the electronic and lattice components of the specific heat, there appears in the semimetals a term due to the interaction of the nuclear electric quadrupole moment with the electric field gradient of the crystal. It is known[37] that this contribution to first order in $1/T$ has a $T^{-2}$ temperature dependence

$$C_Q=\frac{R}{80}\frac{(2I+2)(2I+3)}{2I(2I-1)}\left(\frac{e^2qQ}{KT}\right)^2=\alpha T^{-2}, \qquad (29)$$

where $R$ is the universal gas constant, $I$ is the nuclear spin, $q$ is the largest component of the electric-field-gradient tensor in the principal-axis system, and $Q$ is the scalar quadrupole moment of the nucleus.

The electronic component is expected from free-electron theory to be linear in $T$ to first order;

$$C_e=\tfrac{1}{3}\pi^2K^2TZ+O(T^3)\rightarrow\gamma T, \qquad (30)$$

and for the lattice contribution, the low-temperature Debye approximation of Eq. (15) will be used:

$$C_g\approx(12\pi^4NK/5)(T/\Theta)^3=\beta T^3. \qquad (31)$$

The total specific heat of the sample can thus be written as the sum of the three contributions,

$$C=\alpha T^{-2}+\gamma T+\beta T^3,$$

and for purposes of analysis one writes

$$C/T=\alpha T^{-3}+\beta T^2+\gamma. \qquad (32)$$

The specific-heat data were analyzed in the following manner: The heat capacity of the sample and its addenda were measured and normalized to $C$ using the final weight of the sample. The value of the apparent coefficients $\alpha'$, $\beta'$, and $\gamma'$ for the separate contributions were determined by fitting the data points plotted in $C/T$ versus $T^2$ to an equation of type (32). The experimental points are shown in Fig. 6 (upper part) where the solid line represents the result of a least-squares fit. In a separate experimental run the heat capacity of the addenda (i.e., the holder, thermometers, heater, and the residual piece of the antimony metal) was determined and normalized in the same manner, and the coefficients $\alpha''$, $\beta''$, and $\gamma''$ appropriate to this data were found. The experimental points are shown in Fig. 6 (lower part) where the solid line represents the result of a least-squares fit. The coefficients characteristic of the antimony sample alone were then obtained by subtraction of the two sets of coefficients. The values obtained are listed in Table I and are compared to the other recently determined values. The measured value for the nuclear-quadrupole contribution $\alpha T^{-2}$ is found to be $(1.97\pm0.23)T^{-2}$ $\mu$J deg$^{-1}$ mole$^{-1}$. This value differs by more than a factor of 2 from that of McCollum and Taylor[38] as shown in Table I; both ranges of error are relatively large. Lower temperatures were used in this work than in the work of Ref. 38 and should in principle lead to a more precise determination of $\alpha$. If Eq. (29) and experimentally determined values[39] of $Q$ are used to find

[37] N. E. Phillips, Phys. Rev. **118**, 644 (1960).

[38] D. C. McCollum and W. A. Taylor, Phys. Rev. **156**, 782 (1967).

[39] R. R. Hewitt and B. F. Williams, Phys. Rev. **129**, 1188 (1963); D. Strominger, J. M. Hollander, and G. T. Seaborg, Rev. Mod. Phys. **30**, 697 (1958).

$\alpha$, the results vary widely from 4.37 to 1.9$\mu$J deg$^{-1}$ mole$^{-1}$.

Figure 7 shows the result of the specific-heat curve fit, together with the thermoelectric data expressed in units of $C/T$. The slope of the linear portion of the plot of $C/T$ versus $T^2$ (Fig. 7) is a measure of the Debye temperature $\Theta$, through the relation $\beta=(12/5)\pi^4 NK\Theta^{-3}$. The values $\beta=211.0\pm5.3$ $\mu$J mole$^{-1}$ deg$^{-4}$ and $\Theta=209.6$°K are found and compared to the results of the other authors in Table I. Culbert[40] fitted his data to an equation different from Eq. (32), so that his value for $\beta$ cannot be directly compared; the agreement with Ref. 38 is satisfactory.

Finally, the intercept with the $C/T$ axis in Fig. 7 is a measure of the electronic contribution coefficient $\gamma$, and the value $\gamma=116.5\pm6.4$ $\mu$J mole$^{-1}$ deg$^{-2}$ is found. Accurate measurement of the electronic component of the total heat capacity of antimony (and of the other semimetals) is especially difficult because of its small number of conduction electrons. The lattice heat-capacity term dominates over the electronic term down to very low temperatures and still accounts for 75% of the total at 1.0°K. On the other hand, below 0.5°K one faces the rapidly increasing nuclear-quadrupole contribution. In view of these difficulties, the results for $\gamma$, compared in Table I, can be said to be in rather satisfactory agreement.

Using Eq. (30), a value for the electronic density of states $Z=(1.01\pm0.05)\times10^{33}$ erg$^{-1}$ cm$^{-3}$ is found. Agreement is good with the value $Z=(1.03)\times10^{33}$ erg$^{-1}$/cm$^{-3}$ calculated under quadratic-distribution assumption.[20] It is also in fair agreement with the NE determination $Z=(1.10\pm0.07)\times10^{33}$ erg$^{-1}$ cm$^{-3}$, but, as remarked previously, if the difference between these values is taken seriously it may indicate in the NE the influence of a nonisotropic nonquadratic electron distribution.

## IV. CONCLUSION

Residual resistance being preponderant below 2°K indicates that the main scattering of the electrons is due to impurities. The behavior of the lattice thermal conductivity in the lowest range of temperature indicates that the main scattering of the phonons is due to the electrons, whereas the enhancement in this conductivity above 1.4°K seems to be related to the inability for the phonons with $q>2k_F$ (peripheral phonons) to be scattered by the electrons, and the validity of a characteristic scattering Debye temperature $\Theta^*=(2k_F/q_D)\Theta$ is verified. This interpretation implies that the three phonons normal mixing process is still weak at these temperatures, as expected, and it is therefore thought that the apparent agreement with the Ziman's $T^7$ law in the ratio $\lambda_g/\sigma_i$ is accidental, i.e., not indicative of strong mixing.

The predominance of the phonon-electron scattering is also evident at the appearance of a nearly full phonon drag in the NE effect. The comparison of this term with the lattice specific heat indicates that some discrepancy may be expected from the simplifying concept of isotropic phonon gas. The notion of selective drag is also introduced in relation with the $q<2k_F$ drag condition and the weak-phonon mixing.

The electronic density of states determined from the NE effect matches approximately the value obtained from the electronic specific heat. Should the small discrepancy not be due to simple experimental error it may indicate in the NE term the influence of a nonisotropic, nonquadratic electron distribution.

The NE effect does not seem to carry any trace of the nuclear electric quadrupole terms which appear in the specific heat. The direct measurement of the specific heat is in agreement with other recent direct measurements.

## ACKNOWLEDGMENTS

The authors are indebted to D. C. McCollum and W. A. Taylor for communication of their specific-heat results at a date prior to the beginning of the present work. The help of David Smith and R. Vander Barren is gratefully acknowledged.

[40] H. V. Culbert, Bull. Am. Phys. Soc. **10**, 1104 (1965); Phys. Rev. **157**, 560 (1967). References to previous data on the specific heat of antimony can be found in this article.